



Published in final edited form as:

Hypertension. 2017 June ; 69(6): 1198–1206. doi:10.1161/HYPERTENSIONAHA.117.09123.

Selective Nrf2 Gene Deletion in the Rostral Ventrolateral Medulla Evokes Hypertension and Sympatho-Excitation in Mice

Lie Gao¹, Matthew C. Zimmerman¹, Shyam Biswal², and Irving H. Zucker¹

¹Department of Cellular and Integrative Physiology, University of Nebraska Medical Center
985850 Nebraska Medical Center, Omaha, NE 68198-5850

²Department of Environmental Health and Engineering, Johns Hopkins University Bloomberg
School of Public Health, 615 N. Wolfe St. Baltimore, MD 21205

Abstract

Nuclear factor E2-related factor 2 (Nrf2) is a master transcriptional regulator of redox homeostasis that impacts antioxidant gene expression. Central oxidative stress and reduced antioxidant enzyme expression in the rostral ventrolateral medulla (RVLM) contributed to sympatho-excitation in chronic heart failure. In the current study, we hypothesized that deletion of Nrf2 in the RVLM would increase sympathetic drive and blood pressure. Experiments were carried out in Nrf2 floxed mice treated with microinjection of Lentiviral-Cre-GFP or Lentiviral-GFP into the RVLM. Two weeks after viral administration, Nrf2 message, protein, oxidative stress, cardiovascular function, and sympathetic outflow were evaluated. We found that, (1) Nrf2 mRNA and protein in the RVLM were significantly lower in Cre-mice compared with control GFP-mice. Nrf2-targeted antioxidant enzymes were down-regulated, while reactive oxygen species were elevated. (2) Blood pressure measurements indicated that Cre-mice displayed a significant increase in blood pressure (MAP: 123.7 ± 3.8 vs 100.2 ± 2.2 mm Hg, * $p < 0.05$, $n = 6$), elevated urinary NE concentration (456.4 ± 16.9 vs 356.5 ± 19.9 ng/mL, * $P < 0.05$, $n = 6$), and decreased spontaneous baroreflex gain (Up-sequences: 1.66 ± 0.17 vs 3.61 ± 0.22 ms/mm Hg, * $P < 0.05$, $n = 6$; Down-sequences: 1.89 ± 0.12 vs 2.98 ± 0.19 ms/mmHg, * $P < 0.05$, $n = 6$). (3) Cre-mice displayed elevated baseline renal sympathetic nerve activity and impaired inducible baroreflex function. These data suggest that Nrf2 gene deletion in the RVLM elevates blood pressure, increases sympathetic outflow, and impairs baroreflex function potentially by impaired antioxidant enzyme expression.

Keywords

oxidative stress; blood pressure; sympathetic regulation; arterial baroreflex; brainstem

Address Correspondence to: Irving H. Zucker, Ph.D., Department of Cellular and Integrative Physiology, University of Nebraska Medical Center, 985850 Nebraska Medical Center, Omaha, Nebraska 68198-5850, Tel: (402) 559 7161, FAX: (402) 559 4438, izucker@unmc.edu.

Disclosures

None

Introduction

Maintaining redox homeostasis is essential for normal physiological function. Increased production of reactive oxygen species (ROS) and/or impaired antioxidant defense mechanisms result in accumulation of ROS and oxidative stress; well-documented to contribute to the pathogenesis of several chronic cardiovascular diseases, including heart failure and hypertension^{1, 2}. The central nervous system is highly vulnerable to oxidative stress where excessive ROS can evoke oxidative modification of neuronal constituents, such as nucleic acids, lipids, and proteins, leading to acute and chronic functional and structural abnormalities^{3, 4}. Previous data from our group demonstrated that elevated ROS in the rostral ventrolateral medulla (RVLM), the site of pre-sympathetic neurons projecting to the spinal cord⁵, contributes to sympatho-excitation in a rabbit model of chronic heart failure⁶. In addition, redox imbalance in the RVLM has also been suggested to underlie the sympatho-excitation associated with hypertension⁷.

Antioxidant enzyme activity is the principal endogenous defense mechanism protecting cells and organs against oxidative damage by converting the highly reactive oxygen molecules ($O_2^{\bullet -}$ and H_2O_2) into inert products (O_2 and H_2O). In response to an oxidant challenge, antioxidant enzymes are dynamically upregulated at both the transcriptional and translational levels. Nuclear factor erythroid 2-related factor 2 (Nrf2) plays an important role in mediating the transcriptional regulation of many antioxidant enzymes⁸. Under basal conditions, Nrf2 is sequestered in the cytoplasm in association with Kelch-like ECH associating protein 1 (Keap1) resulting in degradation of Nrf2 by ubiquitination mediated by the Cullin3-based E3 ubiquitin ligase complex^{9, 10}. In response to various forms of oxidant stress the cysteine residues of Keap1 are oxidized and the Nrf2-Keap1 complex is disrupted, facilitating translocation of Nrf2 to the nucleus where it binds to the antioxidant responsive elements (AREs) in the promoter region of multiple genes, leading to upregulation of a battery of antioxidant enzymes, including superoxide dismutase (SODs), NAD(P)H:quinone oxidoreductase 1 (NQO1), heme oxygenase 1 (HO-1), and Catalases^{11, 12}.

Although decreased antioxidant enzymes have been well recognized as a major contributor to the central oxidative stress and sympathetic hyperactivity in heart failure and hypertension^{6, 13, 14}, the mechanisms underlying the down-regulation of these antioxidant enzymes are largely unknown. Furthermore, the roles of Nrf2 in central redox homeostasis and sympathetic regulation remain to be elucidated. Therefore, in the present study, we employed an Nrf2 floxed mouse model to determine if deletion of the Nrf2 gene specifically in the RVLM alters blood pressure and sympathetic outflow in otherwise normal mice. We hypothesized that mice with impaired Nrf2 signaling in the RVLM will exhibit an increase in sympathetic tone and blood pressure.

Materials and Methods

Forty-nine Nrf2 floxed ($Nrf2^{flox/flox}$) mice (28 males and 21 females) aged between 16 – 20 weeks were used in these experiments. Mice were originally obtained from Dr. Shyam Biswal at the Johns Hopkins University¹⁵. All experiments were approved by the Institutional Animal Care and Use Committee of the University of Nebraska Medical Center

and were carried out under the guidelines of the National Institutes of Health *Guide for the Care and Use of Laboratory Animals*.

Induction of RVLM-Specific Nrf2 Deficiency

The Nrf2 gene of the Nrf2^{fllox/fllox} mice was modified by inserting two loxP sites flanking Exon 5. Excision was accomplished by microinjection of lentiviral Cre-recombinase, thus generating a Nrf2 deficiency model¹⁵. To selectively delete the Nrf2 gene in the RVLM, Lentiviral-Cre-GFP (Lentiviral-GFP as the control; 1×10^8 TU/mL, 20 nL; Kerafast, Inc. Boston MA) was injected bilaterally into the RVLM of Nrf2^{fllox/fllox} mice (referred to as Cre-mice and GFP-mice) employing a mouse stereotaxic instrument (SR-5M-HT, NARISHIGE International USA, INC, Amityville, NY) under isoflurane anesthesia (~2%), using the coordinates: 1.2 mm lateral to the midline, 5.3 mm ventral to the dorsal surface of the brain, 1.9 mm caudal to lambda¹⁶. This lentiviral vector includes both 5' and 3' lentiviral LTR and all necessary elements for effective transduction and expression of the Cre and/or GFP genes, driven by the Cytomegalovirus (CMV) promoter. Two to three weeks after injection, the mice underwent chronic recording in the conscious state and acute experiments under anesthesia, followed by euthanasia with an overdose of pentobarbital sodium (150 mg/kg, ip). The brainstem was removed and stored at -80 °C for subsequent biochemical measurements.

Chronic Experiments in Conscious State

Blood Pressure Telemetry Implantation—Under aseptic conditions and isoflurane anesthesia (~2%), a radiotelemetry unit (PA-C10, Data Science International; St Paul, MN) was subcutaneously secured in the neck-back area between the scapulae, with the catheter inserted into the aorta through right common carotid artery.

Blood Pressure (BP) and Heart Rate (HR) Recording—One week after telemetry surgery, BP was continuously recorded for 3 days at a sampling rate of 1 kHz using a PowerLab data acquisition system (model 8S; ADInstruments; Colorado Springs, CO). Heart rate was derived from the arterial pressure pulse.

Spontaneous Baroreflex Sensitivity (SBRS) Analysis—SBRS was elicited from the recorded pulsatile BP signals based on the sequence technique¹⁷⁻¹⁹, using the freely available HemoLab Software (Version 20.2, Dr. Harald M. Stauss Lab, the University of Iowa). After loading the hemodynamic tracing into the program, individual sequences of increases or decreases in BP in mmHg (x-axis) and pulse interval in msec (y-axis) values were plotted and subjected to linear regression. The average of the slopes of all individual regression lines were then used as an index of baroreceptor-heart rate reflex sensitivity (ms/mmHg).

Acute Experiments

Blood Pressure, Heart Rate, and Renal Sympathetic Nerve Activity (RSNA) Recording—Under urethane (800 mg/kg) and α -chloralose (40 mg/kg) anesthesia, the trachea was cannulated and connected to a mouse ventilator (tidal volume: 150 μ L, frequency: 200 breaths/min). The right carotid artery was dissected, and a catheter-tipped

transducer (SPR-1000, Millar Instruments, Houston, TX,) was advanced into the ascending aorta for recording of BP and HR. The right femoral vein was cannulated for saline supplementation and administration of vasoactive agents when baroreflex sensitivity was evaluated. A bundle of left renal sympathetic nerves was isolated in the retroperitoneal space through a left flank incision and placed on a pair of platinum-iridium electrodes. The nerve-electrode complex was covered with silicone gel (Kwik-Sil, WPI, Sarasota FL). The RSNA signal was amplified ($\times 1000$) and filtered (bandwidth: 30–3,000 Hz) using a Grass P55C preamplifier, and then was input into a PowerLab[®] data-acquisition system, from which the signal was monitored, recorded, and saved in a computer using the LabChart[®] 7 software.

Baseline RSNA and Induced Baroreflex Sensitivity (IBRS) and Analysis—After recording approximately 20 minutes of stable baseline hemodynamics and RSNA, phenylephrine (PE) was administered ($0.2\mu\text{g}/\mu\text{L}$ in 20–40 μL , iv) to increase BP. The resultant bradycardia and sympatho-inhibition were continuously recorded. Mice were then euthanized and the maximum RSNA was obtained within 1–2 min, followed by a recording of background noise approximately 15–20 min after death. Baseline RSNA was determined as the percent of maximum RSNA activity after the background noise was subtracted.

The IBRS was analyzed by logistic regression over the entire pressure range after PE administration. The values of BP and RSNA were acquired every 2 seconds from the threshold to the saturation points. A sigmoid logistic regression curve was fit to the data points using the following equation: $\text{RSNA} = A / \{1 + \exp[B(\text{MAP} - C)]\} + D$; where A is the RSNA range, B is the slope coefficient, MAP is the mean arterial pressure, C is the pressure at the midpoint of the range (BP_{50}), and D is the minimum RSNA²⁰. The peak slope (or maximum gain) was determined by taking the first derivative of the baroreflex curve and was calculated with the equation: $\text{Gain max} = A(1) \times A(2) \times [1/4]$, where A(1) is the range and A(2) is the average slope. The mean values for each curve parameter were used to derive composite curves for each experimental group.

Biochemical and Molecular Measurements

Urinary NE—To collect urine, mice were placed in a metabolic cage (Harvard Apparatus, Holliston, MA). Daily food/water intake and urine/fecal excretion were measured.

Urinary NE was measured using a Norepinephrine Enzyme Immunoassay kit (Labor Diagnostika Nord KG, Nordhorn, Germany). A 50- μL urine sample was diluted with 950 μL double-distilled H_2O to obtain a 20:1 diluted sample, from which 10 μL was used for NE measurements based on the instructions provided by the company. Duplicate measurements were made for each sample. 24-hour NE excretion was calculated by multiplying NE concentration by 24-hour urine volume.

Evaluation of Oxidative Stress

i) Dihydroethidium (DHE) Staining: The unfixed frozen mouse brainstem was cut into 30 μm sections and placed on glass slides, which were immersed in 2×10^{-6} M DHE diluted with DMSO and acetone. After incubation in a light-protected, humidified chamber at 37°C for 30 min, extra staining solution was removed, followed by 3 rinses with PBS. The

fluorescence generated by oxidized DHE was detected using a laser confocal microscope (Leica TSC STED) using 488 nm excitation wavelength and a 585-nm filter. The relative fluorescent intensity of images was quantified using Image-J software (National Institutes of Health).

ii) Electron Paramagnetic Resonance (EPR) Spectroscopy: To obtain ample amount of tissue for EPR spectroscopy, eight RVLM punches from four GFP-mice or Cre-mice were pooled into a single EPR sample. Immediately after sample collection, RVLM punches were incubated with a superoxide-sensitive EPR spin probe, 1-hydroxy-3-methoxycarbonyl -2,2,5,5-tetramethylpyrrolidine (CMH), for 60 minutes at 37°C in EPR incubation buffer consisting of (in mM): 99 NaCl, 4.69 KCl, 2.5 CaCl₂, 1.2 MgSO₄, 25 NaHCO₃, 1.03 KH₂PO₄, 5.6 D-glucose, 20 HEPES and supplemented with the metal chelators DETC (5 µM) and DF (25 µM). Samples were then loaded into a 1-cc syringe and flash frozen between EPR buffer solutions to form a continuous frozen plug using liquid nitrogen. The frozen EPR sample plug was then placed into a liquid nitrogen finger dewar and inserted into a Bruker eScan EPR Spectrometer. The following EPR spectrometer settings were used: field sweep width, 100.0 G; microwave frequency, 9.75 kHz; microwave power, 1.10 mW; modulation amplitude, 5.94 G; conversion time, 10.24 ms; time constant, 40.96 ms. It should be noted that the EPR spectrum obtained from the GFP and Cre-mice RVLM samples were normalized to the total weight (mg) of tissue in each sample.

mRNA and Protein Expression

i) Real-time RT-PCR: Total RNA was extracted from the RVLM punches (coordinates: 1.25–1.75 mm lateral to the midline, 1.25–2.00 mm ventral to the dorsal surface of the brainstem, 1.16–1.52 mm cranial from the obex¹⁶) with TRIZOL reagent (Invitrogen), which was then reverse transcribed into double-stranded cDNA using an iScript cDNA synthesis kit (Bio-Rad Laboratories). Templates (50 ng cDNA) were subjected in triplicate to real-time PCR using a thermocycler (PTC-200 Peltier thermal cycler with CHROMO4 continuous fluorescence detector; Bio-Rad Laboratories) and Brilliant III Ultra-Fast QPCR master mix (Agilent Technologies). Specific primers of mouse Nrf2 (Mm.PT.58.29108649) and glyceraldehyde-3-phosphate dehydrogenase (GAPDH; Mm.PT.39a.1) from the Integrated DNA Technologies (Coralville, Iowa) were used for semi-quantification of Nrf2 mRNA expression. Nrf2 mRNA was first normalized against GAPDH mRNA as cycle threshold, and then the relative expression was compared to the control group using the cycle threshold method for quantification with Opticon Monitor software (Bio-Rad Laboratories).

ii) Western Blotting: The target proteins and their primary antibodies were Nrf2 (ab31163 R-IgG), NQO1 (sc-376023 M-IgG), HO-1 (sc-10789 R-IgG), SOD2 (sc-30080 R-IgG), and Catalase (sc-34280 G-IgG). GAPDH (sc-32233 M-IgG) served as an internal control. RVLM punches were homogenized in RIPA buffer, and total protein was extracted from the homogenates. Protein concentration was measured using a protein assay kit and then adjusted by adding 4% sodium dodecyl sulfate sample buffer to obtain equal concentrations among these samples. The samples were then loaded on a 10% SDS-PAGE gel (30 µg protein per well) and subjected to electrophoresis. The fractionized protein on the gel was

electrically transferred onto a polyvinyl difluoride membrane. The membrane was first probed with the primary antibody to the target protein and then with GAPDH primary antibody. After incubation with primary antibodies, the membranes were probed with secondary antibodies followed by treatment with enhanced chemiluminescence substrate (Pierce). The bands on the membrane were visualized and analyzed using a UVP BioImaging System. The final reported data are the target protein band densities divided by the GAPDH density.

iii) Immunofluorescence Staining: The area of Nrf2 deletion in the Cre-mouse RVLM was confirmed using immunofluorescence staining. Mice were deeply anesthetized with sodium pentobarbital and perfused transcardially with PBS, followed by perfusion of 4% paraformaldehyde in PBS. The entire brainstem was removed, mounted on a specimen stage, and sectioned into 40- μ m slices in a cryostat. The slices were then washed with PBS 3 times and permeabilized for 30 minutes at room temperature with a solution containing 0.3% Triton X-100 dissolved in PBS, followed by blocking with solution containing 10% normal goat serum and 0.3% Triton X-100 in PBS at room temperature for 2 hours. The slices were then incubated with Nrf2 antibody (ab31163 R-IgG), in 10% normal goat serum and 0.3% Triton X-100 in PBS at 4°C overnight. After three washes with PBS, the slices were incubated for 2 hours with secondary fluorescent antibody (Goat anti-Rabbit IgG secondary antibody, Alexa Fluor 546; Invitrogen, A-11010). The slices were mounted with an Aqua-Mount Mounting Medium, and then were examined with a laser confocal microscope (Leica TSC STED).

Statistical analyses

All of the data are expressed as mean \pm SE. Student t test was used to compare the difference between two groups, with the aid of SigmaPlot software. A P value of <0.05 was taken as indicative of statistical significance.

Results

Nrf2 mRNA and Protein Expression

Nrf2 mRNA and protein expression in the RVLM of Nrf2^{flox/flox} mice 2 – 3 weeks after bilateral microinjection of Lentiviral-GFP (GFP) and Lentiviral-Cre-GFP (Cre) was determined (Figure 1A and B). Compared with GFP-mice, Cre-mice exhibited significantly lower Nrf2 mRNA (Panel A, 0.30 ± 0.08 vs 1.00 ± 0.11 , $**p < 0.01$, $n = 7$) and protein (Panel B, 0.07 ± 0.02 vs 0.32 ± 0.03 , $**p < 0.01$, $n = 7$) in RVLM punches. These data indicate a transcriptional and translational downregulation of Nrf2 in the RVLM of Cre-mice, suggesting that Cre-recombinase excised the Nrf2 gene from the genome leading to a decrease in Nrf2 mRNA, following by a decrease translation of Nrf2 protein. While Nrf2 mRNA and protein were not reduced to zero we believe the traces of Nrf2 mRNA and protein may be due to contamination in the vicinity of the RVLM punches rather than incomplete knockout of the Nrf2 gene within RVLM. Panel C of figure 1 shows immunofluorescence images of Nrf2 protein in one brainstem section at the RVLM level of a Nrf2^{flox/flox} mouse whose right RVLM was injected with Lentiviral-Cre-GFP and left RVLM was intact as the control. The area of injection into the RVLM shows a strong GFP

signal however very low or absence of a red Nrf2 immuno-positive signal, suggesting selective deletion of Nrf2 in the neurons infected by Lentiviral-Cre-GFP. Importantly, we could find no evidence of GFP staining in other areas of the brainstem and hypothalamus. Therefore, we believe that these injections selectively deleted the Nrf2 gene in the RVLM.

Expressions of Nrf2 Downstream Target Proteins

Western blot data (Figure 2) shows protein expression of Nrf2 downstream targets, the antioxidant enzymes, in RVLM punches of GFP-mice and Cre-mice. NQO1, HO1, SOD2 and Catalase were all reduced in the tissue from Cre-mice compared with the GFP-mice (NQO1: 0.37 ± 0.08 vs 1.12 ± 0.10 , $**p < 0.01$; HO-1: 0.33 ± 0.10 vs 0.90 ± 0.12 , $**p < 0.01$; SOD2: 0.52 ± 0.12 vs 0.92 ± 0.11 , $*p < 0.05$; Catalase: 0.66 ± 0.12 vs 1.27 ± 0.13 , $*p < 0.05$. $n = 7$ in each group), suggesting that Nrf2 gene deletion also leads to a downregulation of a battery of antioxidant enzymes.

Oxidative stress measurements

Figure 3 shows the superoxide level in the RVLM of GFP-mice and Cre-mice. Panel A represents DHE staining showing a stronger red fluorescent signal and higher quantified density of red fluorescence in RVLM of Cre-mice as compared to GFP-mice (71.8 ± 3.0 vs 39.2 ± 1.7 , $*p < 0.05$, compared to GFP-mice, $n = 6$ for each group). Panel B shows EPR spectra obtained from fresh RVLM punches pooled from 4 GFP-mice and 4 Cre-mice following incubation with the superoxide-sensitive EPR spin probe, 1-Hydroxy-3-methoxycarbonyl-2,2,5,5-tetramethylpyrrolidine HCl (CMH). Upon reacting with superoxide, the CMH spin probe becomes a stable nitroxide radical, which when placed in the appropriate magnetic field scan (Gauss) yields the characteristic spectra shown in Figure 3B²¹. Notably, each spectrum was normalized to the total weight (mg) of tissue in the respective sample. Considering the amplitude of the EPR spectrum is directly proportional to the levels of superoxide in the sample²¹, the enhanced EPR spectrum amplitude obtained from Cre-mice RVLM punches compared to that from GFP-mice RVLM punches indicates an increase in superoxide levels in the RVLM of Cre-mice. Collectively, these data suggest that, in the RVLM, Nrf2 deletion results in an increase in reactive oxygen species, particularly superoxide.

Cardiovascular Sympathetic Regulation in the Conscious State

Measurements of BP and sympathetic tone were carried out in order to assess the systemic effects of RVLM Nrf2 deletion. Figure 4, panel A shows BP and HR data grouped by 1-hour averages (left) and 24-hour average data (right). GFP-mice and Cre-mice exhibited a similar circadian rhythm of BP and HR. Blood pressure in Cre-mice was elevated in both nighttime and daytime compared to GFP-mice (24-hour average MAP: 123.7 ± 3.8 vs 100.2 ± 2.2 mm Hg, $*p < 0.05$, $n = 6$), whereas there was no difference in HR between these two groups (24-hour average HR: 531.2 ± 13.9 vs 536.1 ± 14.3 bpm, $n = 6$). No differences in BP or HR response were observed between male and female mice (data not shown). Panel B shows the spontaneous arterial baroreflex sensitivity (SBRS) evaluated in the conscious state. Both up-sequence gain (1.66 ± 0.17 vs 3.61 ± 0.22 ms/mm Hg, $*P < 0.05$, $n = 6$) and down-sequence gain (1.89 ± 0.12 vs 2.98 ± 0.19 ms/mmHg, $*P < 0.05$, $n = 6$) were significantly decreased in Cre-mice as compared to the GFP-mice, suggesting impaired arterial baroreflex function in

mice with Nrf2 deficiency in RVLM. In addition, both urinary NE concentration (456.4 ± 16.9 vs 356.5 ± 19.9 ng/mL, $*P < 0.05$, $n = 13-14$) and 24-hour NE excretion (676.5 ± 64.2 vs 416.5 ± 28.1 ng/24h, $*P < 0.05$, $n = 13-14$) were higher in Cre-mice, suggesting a sympatho-excitatory effect of RVLM Nrf2 knockdown in the Cre-mice. However, there was no difference in water/food intake or urine/fecal excretion between these two groups (data not shown).

Cardiovascular and Sympathetic Regulation in the Anesthesia State

Figure 5 shows the renal sympathetic nerve activity (RSNA) and induced arterial baroreflex sensitivity (IBRS) in GFP-mice and Cre-mice in the anesthetized state. Baseline BP, HR, and RSNA are shown in Panel A (top: original recording; bottom: mean data). Cre-mice exhibited significantly higher baseline RSNA as compared to the GFP-mice (63.8 ± 8.1 vs 24.2 ± 4.3 % of max, $**P < 0.01$ vs GFP-mice, $n = 6$ for each group). Panel B shows arterial baroreflex data original recording (left, top), composite baroreflex curves (right, top, insert is the gain of IBRS), and the five parameters reflecting IBRS sensitivity (bottom). The representative recording shows transient silencing of RSNA and a profound decline of HR when the BP was increased by PE administration in a GFP-mouse, whereas the decrease of RSNA and HR to the PE-evoked hypertension was markedly blunted in Cre-mice, suggesting an impairment of baroreflex function in mice with Nrf2 deletion in the RVLM. Indeed, the bottom graphs of Panel B in Figure 5 show that the average slope (0.083 ± 0.01 vs 0.119 ± 0.01 % of mm Hg, $**P < 0.01$), maximal gain (1.64 ± 0.20 vs 2.66 ± 0.20 % of mm Hg, $**P < 0.01$), and range of RSNA response of baroreflex (69.9 ± 6.8 vs 89.4 ± 8.4 % of max, $*P < 0.05$) were significantly decreased, whereas the BP_{50} (102.3 ± 8.9 vs 80.1 ± 11.5 mm Hg, $*P < 0.05$) and minimum RSNA of baroreflex (23.32 ± 5.5 vs 9.0 ± 1.2 % of max, $*P < 0.05$) were significantly higher in Cre-mice compared with GFP-mice ($n = 6$ for each group).

Discussion

Redox homeostasis is an essential function maintaining the “milieu intérieur” in the physiologic state²². It has been well-recognized that central oxidative stress plays a crucial role in maladaptive cardiovascular function and sympathetic outflow in chronic heart failure² and hypertension¹. Excessive central, especially brainstem and hypothalamic, ROS in cardiovascular disease is derived from an imbalance between pro-oxidative and antioxidant processes²³. This imbalance results in intracellular and perhaps extracellular ROS accumulation, leading to neural dysfunction²⁴. Indeed, in heart failure and hypertension, NADPH oxidase has been shown to be activated and SODs downregulated in key cardiovascular nuclei, such as the RVLM thus contributing sympatho-excitation^{25, 26}.

In the present study we determined if selective deletion of the antioxidant enzyme transcription factor Nrf2 in the RVLM altered sympathetic nerve activity and blood pressure in normal mice. By employing Nrf2^{flox/flox} mice and using lentiviral-Cre-GFP microinjection, we successfully deleted the Nrf2 gene in the RVLM, resulting in a decrease in Nrf2 mRNA and protein expression, which lead to a downregulation of antioxidant enzymes and elevation of ROS. The most profound finding in this study was a significant

elevation of blood pressure associated with an increase in urinary NE concentration and excretion, elevated renal sympathetic nerve activity, and a blunted arterial baroreflex control of HR in the conscious state (SBRS) and suppression of sympathetic nerve activity in the anesthetized state (IBRS). These findings strongly suggest that, in the RVLM of normal mice, Nrf2 gene deficiency contributes to ROS generation, sympatho-excitation and hypertension.

The RVLM is considered to be one of the major brainstem nuclei where pre-sympathetic neurons project to the spinal cord and regulates sympathetic outflow and thus cardiovascular function^{27, 28}. In addition, projections from other mid-brain, hypothalamic and brainstem nuclei such as subfornical organ (SFO), hypothalamic paraventricular nucleus (PVN) and median preoptic nucleus (MnPO)²⁹, converge on the RVLM where projections to the intermediolateral (IML) cell columns of the spinal cord providing sympathetic preganglionic neurons to the periphery³⁰. The RVLM also receives inhibitory input originating from peripheral reflexes and projections from the nucleus tractus solitarius (NTS) and caudal ventrolateral medulla (CVLM), thus modulating the arterial baroreflex regulation on heart rate and sympathetic nerve activity³¹.

Neurons in the RVLM are susceptible to increased ROS. Sympatho-excitation in several rat models of hypertension has been attributed to oxidative stress in the RVLM²⁶. Indeed, in spontaneous hypertensive rats (both SHR and SHRSP)^{32, 33} and in secondary hypertension (high salt-, obesity-, and jet leg-induced)³⁴⁻³⁶, superoxide levels in the RVLM are increased, contributing to sympatho-excitation and the elevated blood pressure. In previous studies from our laboratory we showed increased oxidative stress in the RVLM in rabbits with heart failure that was responsible for augmented sympatho-excitation^{6, 25, 37}. The mechanism(s) by which this increased sympatho-excitation takes place has not been completely defined.

The present data showing sympatho-excitation and hypertension in mice after Nrf2 knockdown in the RVLM suggests a tonic production of ROS in this critical sympathetic nucleus under physiological conditions, and that oxidant stress can evoke cardiovascular and sympathetic dysfunction of a sustained nature. The source of ROS in the RVLM is not completely clear. Potential pro-oxidative mechanisms in brain include nicotinamide adenine dinucleotide phosphate (NADPH) oxidase, xanthine oxidase, uncoupled nitric oxide synthase, and mitochondria³⁸⁻⁴⁰. NAD(P)H oxidase is a major contributor to superoxide generation in the RVLM, especially in response to activation of the Angiotensin II-AT1R signaling pathway which is activated in hypertension and CHF^{6, 41}. It is not clear if a pre-synaptic or post-synaptic mechanism, or both mediate ROS modulation of sympathetic nerve activity in the RVLM. In the RVLM of SHR, it has been demonstrated that ROS improved the release of the excitatory amino acid glutamate while suppressed the release of the inhibitory amino acid GABA³³. On the other hand, in rats with coronary artery ligation induced heart failure, we documented that increased superoxide mediated Angiotensin II-induced downregulation of the potassium channel protein, Kv4.3 expression and increase in neuronal excitability in the RVLM⁴². In dissociated neurons from rat hypothalamus and brainstem, Angiotensin II-induced ROS decreased potassium channel opening, leading to an inhibition of a delayed rectifying potassium current and membrane depolarization⁴³. These studies suggest that both pre-synaptic and post-synaptic mechanisms are responsible for

ROS neuronal modulation in the RVLM to induce sympatho-excitation. Glia are another potential source of ROS in the RVLM. Recently, crosstalk between glial cells and presympathetic neurons within RVLM and sympathetic tone have been demonstrated⁴⁴. Although the functional implication of ROS in this process is lacking, the potential involvement of glial cells in the maladaptive sympathetic regulation seen in these Nrf2 deficient mice cannot be excluded. While we did not specifically examine glia in the RVLM in this study, the immunofluorescent images and DHE staining show that RVLM neurons are at least one source of increased ROS following Lentiviral-Cre microinjection. All of the RVLM neurons responsible for sympathetic regulation and directly innervating sympathetic preganglionic neurons of IML are glutaminergic, among which ~70% neurons also synthesize adrenaline, defined as the C1 group^{28, 45, 46}. One limitation of the present study is that we cannot discriminate the neuronal subtypes where Nrf2 was deleted by Lentiviral-Cre.

Nrf2 is a master regulator of a battery of antioxidant enzymes and plays a central role in protecting cells against oxidant damage in a variety of organs and tissues, including the central nervous system⁴⁷. The significantly lower protein expression of NQO1, HO-1, SOD2, and catalase and elevated ROS level in the RVLM of mice with Nrf2 knockdown seen in the present study further confirms this concept. Given dynamic and aggressive activation in response to oxidative stress, Nrf2 may represent a critical adaptive mechanism to maintain central redox balance. In neurogenic hypertension or other chronic cardiovascular diseases characterized by sympatho-excitation, the central redox balance shifts to the pro-oxidative side^{6, 13, 32} which, in turn, evokes antioxidant defenses. Several key antioxidant enzymes in the RVLM of these diseases have been documented to be down-regulated^{6, 13, 32}, suggesting a maladaptation of oxidative stress perhaps due to the impaired Nrf2 signaling. Accordingly, it will be important to evaluate Nrf2 expression and to determine if impaired Nrf2 signaling contributes to the redox imbalance in the RVLM under these pathological conditions. If so, activation of Nrf2 signaling selectively in the RVLM may be a novel therapeutic strategy for hypertension and chronic heart failure. However, it has not been established that NQO1 and HO-1 expressions are altered in the RVLM of hypertensive and chronic heart failure animals. In a recent study by Wu et al.⁴⁸ it a suppressed Nrf2 function in the RVLM of hypertensive rats induced by lipopolysaccharide, leads to a defect in mitochondrial biogenesis and contributes to the pathogenesis of hypertension. However, in the current study, it is not clear if mitochondrial function was altered and contributed to the elevated blood pressure in mice with Nrf2 deficiency.

Lenti-Cre treated mice in the current study exhibited reduced arterial baroreflex sensitivity. An appropriate baroreflex depends on the functional integrity of baroreceptor afferents, central neural circuits (NTS, CVLM, and RVLM), efferent pathways (parasympathetic and sympathetic nerves), and effector organs (heart and blood vessels)⁴⁹. The blunted baroreflex sensitivity in Nrf2 deficient mice in this study is most likely due to efferent dysfunction originating in the RVLM. We found no GFP fluorescence outside of the RVLM following lenti-Cre microinjection. As indicated above, there is support for the notion that increased ROS can enhance glutamate release⁵⁰ and reduce GABA release³³. The current data does not allow us to establish a causal relationship between baroreflex dysfunction, sympatho-excitation, and hypertension in mice where Nrf2 has been knocked down in the RVLM.

However, it is clear that the hypertension in these mice was associated with an increase in sympathetic outflow. Interestingly, there was no change in HR following lenti-Cre administration. While it is not clear why HR did not increase as did BP, it may be that the high level of cardiac sympathetic tone in mice represents a ceiling effect so that further increases are unlikely. Indeed, cardiac sympathetic tone in mice is significantly higher compared with rats, whereas vascular sympathetic tone is similar in these two species⁵¹. Given that mice have a limited reserve to increase cardiac output⁵¹, vasoconstriction induced increase in peripheral resistance is likely the predominant contributor to the hypertension seen in these RVLM Nrf2 knockout mice.

In summary, we show here that selective deletion of the Nrf2 gene in the RVLM of mice results in a remarkable decrease in Nrf2 mRNA and protein expression, leading to a downregulation of HO-1, NQO1, SOD2, and catalase protein expression, and an elevation of superoxide and ROS in the RVLM. This mouse model displays sustained hypertension, sympatho-excitation, and baroreflex dysfunction. These data suggest that Nrf2 plays a critical role in the modulation of redox homeostasis in the RVLM, contributing to cardiovascular function and sympathetic regulation.

Perspectives

Essential hypertension is a sympatho-excitatory state that can be difficult to treat. In many cases patients are resistant to pharmacological therapy. Therefore, a search for novel mechanisms that regulate sympathetic nerve activity is of importance. The study reported in this paper focused on the regulation of central antioxidant enzyme expression in normotensive mice following deletion of the Nrf2 gene and protein in the RVLM. The experiments resulted in sympatho-excitation and hypertension. Because oxidative stress is an important regulator of neuronal activity, activation of Nrf2/antioxidant signaling in the brain may be a novel target for therapy in hypertension and other sympatho-excitatory states.

Acknowledgments

We thank Ms Li Yu for her expert technical assistance for both real-time RT-PCR and Western blot analyses.

Sources of Funding

This study was supported by NIH grant P01 HL62222 (IHZ). SB was supported by U01 ES026721. EPR Spectroscopy data were collected in the University of Nebraska's EPR Spectroscopy Core, which is supported, in part, by a grant from the National Institute of General Medical Sciences of the National Institutes of Health (P30GM103335) awarded to the University of Nebraska's Redox Biology Center.

References

1. Peterson JR, Sharma RV, Davison RL. Reactive oxygen species in the neuropathogenesis of hypertension. *Curr Hypertens Rep.* 2006; 8:232–241. [PubMed: 17147922]
2. Zucker IH. Novel mechanisms of sympathetic regulation in chronic heart failure. *Hypertension.* 2006; 48:1005–1011. [PubMed: 17015773]
3. Patel M. Targeting Oxidative Stress in Central Nervous System Disorders. *Trends Pharmacol Sci.* 2016; 37:768–778. [PubMed: 27491897]
4. Friedman, J. *Neurology.* Humana Press; 2011. Oxidative Stress and Free Radical Damage in.
5. Dampney RA, Goodchild AK, Tan E. Identification of cardiovascular cell groups in the brain stem. *Clin Exp Hypertens A.* 1984; 6:205–220. [PubMed: 6365367]

6. Gao L, Wang W, Li YL, Schultz HD, Liu D, Cornish KG, Zucker IH. Superoxide mediates sympathoexcitation in heart failure: roles of angiotensin II and NAD(P)H oxidase. *Circ Res.* 2004; 95:937–944. [PubMed: 15459075]
7. Tai MH, Wang LL, Wu KL, Chan JY. Increased superoxide anion in rostral ventrolateral medulla contributes to hypertension in spontaneously hypertensive rats via interactions with nitric oxide. *Free Radic Biol Med.* 2005; 38:450–462. [PubMed: 15649647]
8. Nguyen T, Sherratt PJ, Nioi P, Yang CS, Pickett CB. Nrf2 controls constitutive and inducible expression of ARE-driven genes through a dynamic pathway involving nucleocytoplasmic shuttling by Keap1. *J Biol Chem.* 2005; 280:32485–32492. [PubMed: 16000310]
9. Cullinan SB, Gordan JD, Jin J, Harper JW, Diehl JA. The Keap1-BTB protein is an adaptor that bridges Nrf2 to a Cul3-based E3 ligase: oxidative stress sensing by a Cul3-Keap1 ligase. *Mol Cell Biol.* 2004; 24:8477–8486. [PubMed: 15367669]
10. Kobayashi A, Kang MI, Okawa H, Ohtsui M, Zenke Y, Chiba T, Igarashi K, Yamamoto M. Oxidative stress sensor Keap1 functions as an adaptor for Cul3-based E3 ligase to regulate proteasomal degradation of Nrf2. *Mol Cell Biol.* 2004; 24:7130–7139. [PubMed: 15282312]
11. Ma Q. Role of nrf2 in oxidative stress and toxicity. *Annu Rev Pharmacol Toxicol.* 2013; 53:401–426. [PubMed: 23294312]
12. Kensler TW, Wakabayashi N, Biswal S. Cell survival responses to environmental stresses via the Keap1-Nrf2-ARE pathway. *Annu Rev Pharmacol Toxicol.* 2007; 47:89–116. [PubMed: 16968214]
13. Chan SH, Tai MH, Li CY, Chan JY. Reduction in molecular synthesis or enzyme activity of superoxide dismutases and catalase contributes to oxidative stress and neurogenic hypertension in spontaneously hypertensive rats. *Free Radic Biol Med.* 2006; 40:2028–2039. [PubMed: 16716903]
14. Kishi T, Hirooka Y, Konno S, Sunagawa K. Sympathoinhibition induced by centrally administered atorvastatin is associated with alteration of NAD(P)H and Mn superoxide dismutase activity in rostral ventrolateral medulla of stroke-prone spontaneously hypertensive rats. *J Cardiovasc Pharmacol.* 2010; 55:184–190. [PubMed: 20040888]
15. Kong X, Thimmulappa R, Craciun F, Harvey C, Singh A, Kombairaju P, Reddy SP, Remick D, Biswal S. Enhancing Nrf2 pathway by disruption of Keap1 in myeloid leukocytes protects against sepsis. *Am J Respir Crit Care Med.* 2011; 184:928–938. [PubMed: 21799073]
16. Franklin, KBJ., Paxinos, G. *The Mouse Brain In Stereotaxic Coordinates.* 360 Park Avenue South, New York, NY, USA: Academic Press; 2007.
17. Baudrie V, Laude D, Elghozi JL. Optimal frequency ranges for extracting information on cardiovascular autonomic control from the blood pressure and pulse interval spectrograms in mice. *Am J Physiol Regul Integr Comp Physiol.* 2007; 292:R904–R912. [PubMed: 17038438]
18. Stauss HM, Moffitt JA, Chapleau MW, Abboud FM, Johnson AK. Baroreceptor reflex sensitivity estimated by the sequence technique is reliable in rats. *Am J Physiol Heart Circ Physiol.* 2006; 291:H482–H483. [PubMed: 16772526]
19. Laude D, Baudrie V, Elghozi JL. Applicability of recent methods used to estimate spontaneous baroreflex sensitivity to resting mice. *Am J Physiol Regul Integr Comp Physiol.* 2008; 294:R142–R150. [PubMed: 17989145]
20. Kent BB, Drane JW, Blumenstein B, Manning JW. A mathematical model to assess changes in the baroreceptor reflex. *Cardiology.* 1972; 57:295–310. [PubMed: 4651782]
21. Dikalov S, Griendling KK, Harrison DG. Measurement of reactive oxygen species in cardiovascular studies. *Hypertension.* 2007; 49:717–727. [PubMed: 17296874]
22. Ursini F, Maiorino M, Forman HJ. Redox homeostasis: The Golden Mean of healthy living. *Redox Biol.* 2016; 8:205–215. [PubMed: 26820564]
23. Rahal A, Kumar A, Singh V, Yadav B, Tiwari R, Chakraborty S, Dhama K. Oxidative stress, prooxidants, and antioxidants: the interplay. *Biomed Res Int.* 2014; 2014:761264. [PubMed: 24587990]
24. Wang X, Michaelis EK. Selective neuronal vulnerability to oxidative stress in the brain. *Front Aging Neurosci.* 2010; 2:1–13. [PubMed: 20552041]
25. Gao L, Wang W, Liu D, Zucker IH. Exercise training normalizes sympathetic outflow by central antioxidant mechanisms in rabbits with pacing-induced chronic heart failure. *Circulation.* 2007; 115:3095–3102. [PubMed: 17548725]

26. Kishi T, Hirooka Y. Oxidative stress in the brain causes hypertension via sympathoexcitation. *Front Physiol.* 2012; 3:1–8. [PubMed: 22275902]
27. Dampney RA. Functional organization of central pathways regulating the cardiovascular system. *Physiol Rev.* 1994; 74:323–364. [PubMed: 8171117]
28. Guyenet PG. The sympathetic control of blood pressure. *Nat Rev Neurosci.* 2006; 7:335–346. [PubMed: 16760914]
29. Coote JH. Landmarks in understanding the central nervous control of the cardiovascular system. *Exp Physiol.* 2007; 92:3–18. [PubMed: 17030558]
30. Kumagai H, Oshima N, Matsuura T, Iigaya K, Imai M, Onimaru H, Sakata K, Osaka M, Onami T, Takimoto C, Kamayachi T, Itoh H, Saruta T. Importance of rostral ventrolateral medulla neurons in determining efferent sympathetic nerve activity and blood pressure. *Hypertens Res.* 2012; 35:132–141. [PubMed: 22170390]
31. Pilowsky PM, Goodchild AK. Baroreceptor reflex pathways and neurotransmitters: 10 years on. *J Hypertens.* 2002; 20:1675–1688. [PubMed: 12195099]
32. Kishi T, Hirooka Y, Kimura Y, Ito K, Shimokawa H, Takeshita A. Increased reactive oxygen species in rostral ventrolateral medulla contribute to neural mechanisms of hypertension in stroke-prone spontaneously hypertensive rats. *Circulation.* 2004; 109:2357–2362. [PubMed: 15117836]
33. Nishihara M, Hirooka Y, Matsukawa R, Kishi T, Sunagawa K. Oxidative stress in the rostral ventrolateral medulla modulates excitatory and inhibitory inputs in spontaneously hypertensive rats. *J Hypertens.* 2012; 30:97–106. [PubMed: 22157590]
34. Koga Y, Hirooka Y, Araki S, Nozoe M, Kishi T, Sunagawa K. High salt intake enhances blood pressure increase during development of hypertension via oxidative stress in rostral ventrolateral medulla of spontaneously hypertensive rats. *Hypertens Res.* 2008; 31:2075–2083. [PubMed: 19098380]
35. Kishi T, Sunagawa K. Experimental ‘jet lag’ causes sympathoexcitation via oxidative stress through AT1 receptor in the brainstem. *Conf Proc IEEE Eng Med Biol Soc.* 2011; 2011:1969–1972. [PubMed: 22254719]
36. Kishi T, Hirooka Y, Ogawa K, Konno S, Sunagawa K. Calorie restriction inhibits sympathetic nerve activity via anti-oxidant effect in the rostral ventrolateral medulla of obesity-induced hypertensive rats. *Clin Exp Hypertens.* 2011; 33:240–245. [PubMed: 21699450]
37. Gao L, Wang W, Li YL, Schultz HD, Liu D, Cornish KG, Zucker IH. Sympathoexcitation by central ANG II: roles for AT1 receptor upregulation and NAD(P)H oxidase in RVLM. *Am J Physiol Heart Circ Physiol.* 2005; 288:H2271–H2279. [PubMed: 15637113]
38. Hirooka Y. Oxidative stress in the cardiovascular center has a pivotal role in the sympathetic activation in hypertension. *Hypertens Res.* 2011; 34:407–412. [PubMed: 21346766]
39. Hirooka Y. Brain perivascular macrophages and central sympathetic activation after myocardial infarction: heart and brain interaction. *Hypertension.* 2010; 55:610–611. [PubMed: 20142562]
40. Hirooka Y. Role of reactive oxygen species in brainstem in neural mechanisms of hypertension. *Auton Neurosci.* 2008; 142:20–24. [PubMed: 18650132]
41. Infanger DW, Sharma RV, Davisson RL. NADPH oxidases of the brain: distribution, regulation, and function. *Antioxid Redox Signal.* 2006; 8:1583–1596. [PubMed: 16987013]
42. Gao L, Li Y, Schultz HD, Wang WZ, Wang W, Finch M, Smith LM, Zucker IH. Downregulated Kv4.3 expression in the RVLM as a potential mechanism for sympathoexcitation in rats with chronic heart failure. *Am J Physiol Heart Circ Physiol.* 2010; 298:H945–H955. [PubMed: 20044444]
43. Sun C, Sellers KW, Sumners C, Raizada MK. NAD(P)H oxidase inhibition attenuates neuronal chronotropic actions of angiotensin II. *Circ Res.* 2005; 96:659–666. [PubMed: 15746442]
44. Marina N, Teschemacher AG, Kasparov S, Gourine AV. Glia, sympathetic activity and cardiovascular disease. *Exp Physiol.* 2016; 101:565–576. [PubMed: 26988631]
45. Ross CA, Ruggiero DA, Park DH, Joh TH, Sved AF, Fernandez-Pardal J, Saavedra JM, Reis DJ. Tonic vasomotor control by the rostral ventrolateral medulla: effect of electrical or chemical stimulation of the area containing C1 adrenaline neurons on arterial pressure, heart rate, and plasma catecholamines and vasopressin. *J Neurosci.* 1984; 4:474–494. [PubMed: 6699683]

46. Schreihof AM, Guyenet PG. Identification of C1 presympathetic neurons in rat rostral ventrolateral medulla by juxtacellular labeling in vivo. *J Comp Neurol.* 1997; 387:524–536. [PubMed: 9373011]
47. Lee JM, Li J, Johnson DA, Stein TD, Kraft AD, Calkins MJ, Jakel RJ, Johnson JA. Nrf2, a multi-organ protector? *FASEB J.* 2005; 19:1061–1066. [PubMed: 15985529]
48. Wu KL, Wu CW, Chao YM, Hung CY, Chan JY. Impaired Nrf2 regulation of mitochondrial biogenesis in rostral ventrolateral medulla on hypertension induced by systemic inflammation. *Free Radic Biol Med.* 2016; 97:58–74. [PubMed: 27223823]
49. Wehrwein EA, Joyner MJ. Regulation of blood pressure by the arterial baroreflex and autonomic nervous system. *Handb Clin Neurol.* 2013; 117:89–102. [PubMed: 24095118]
50. Chan SH, Hsu KS, Huang CC, Wang LL, Ou CC, Chan JY. NADPH oxidase-derived superoxide anion mediates angiotensin II-induced pressor effect via activation of p38 mitogen-activated protein kinase in the rostral ventrolateral medulla. *Circ Res.* 2005; 97:772–780. [PubMed: 16151022]
51. Janssen BJ, Smits JF. Autonomic control of blood pressure in mice: basic physiology and effects of genetic modification. *Am J Physiol Regul Integr Comp Physiol.* 2002; 282:R1545–R564. [PubMed: 12010736]

Novelty and Significance

What Is New?

- For the first-time excision of the Nrf2 gene in the rostral ventro-lateral medulla (RVLM) of normal mice results in chronic hypertension.
- A novel use of the Nrf2 floxed mouse is reported.

What is relevant?

- Hypertension is, in part, mediated by sympatho-excitation.
- Adaptive molecular mechanisms that target oxidative stress in the brain may be important therapeutic targets.

Summary

- These data clearly indicate that targeted deletion of Nrf2, a master regulator of antioxidant gene transcription, increases oxidative stress in the RVLM of normal mice resulting in a decrease in antioxidant gene expression, an increase in sympathetic activation, a decrease in baroreflex sensitivity and sustained hypertension of a magnitude equivalent to chronic infusion of pressor agents (e.g. Angiotensin II).

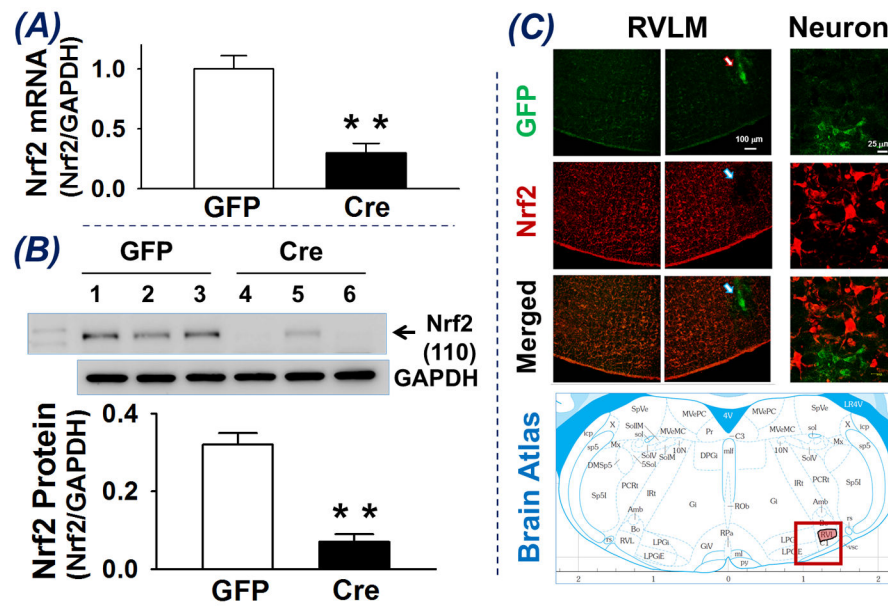


Figure 1. Nrf2 mRNA (A) and Protein (B) expression in RVLM punches of Nrf2^{flox/flox} mice receiving Lentiviral-GFP (GFP) or Lentiviral-Cre-GFP (Cre). **P < 0.01 compared with GFP mice, n = 7 for each group. Panel C is immunofluorescence images of one brainstem section (5.3 mm ventral to the dorsal surface of the brain and 1.9 mm caudal to lambda) from a Nrf2^{flox/flox} mouse whose right RVLM received Lentiviral-Cre-GFP injection. Green is GFP signal indicating the infected region and neurons. Red is Nrf2 immuno-positive signal showing location of Nrf2 protein.

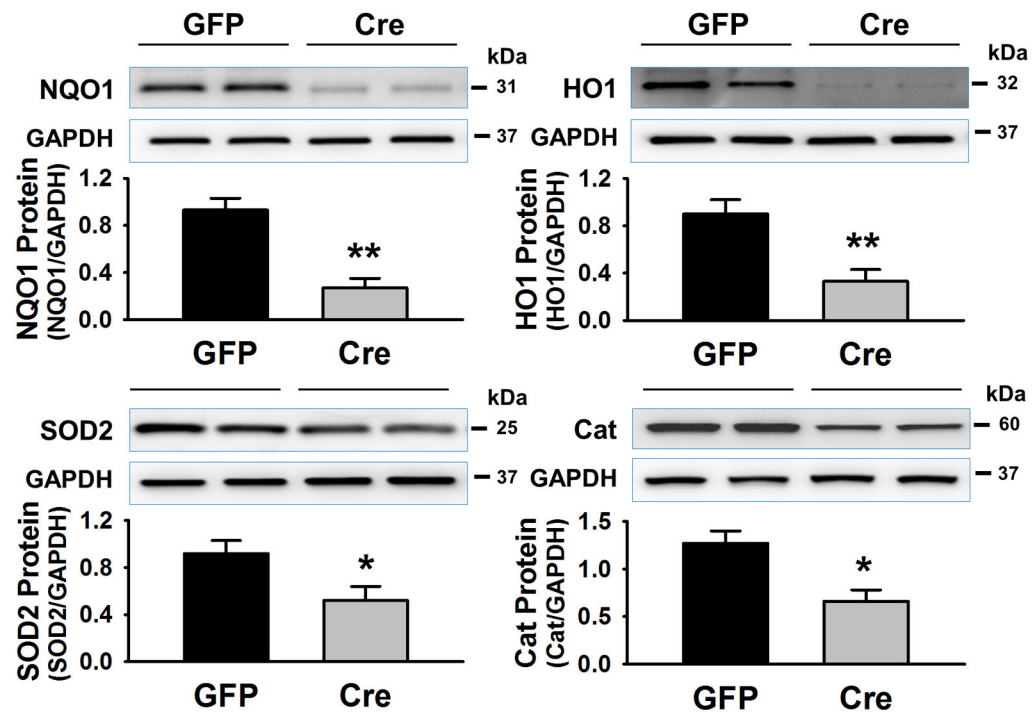


Figure 2. Expressions of Nrf2 downstream target proteins (NQO1, HO-1, SOD2, and Catalase) in the RVLN punches of *Nrf2*^{fllox/fllox} mice with bilateral microinjection of Lentiviral-GFP (GFP) or Lentiviral-Cre-GFP (Cre). **P* < 0.05 and ***P* < 0.01 compared with GFP mice, *n* = 7 for each group.

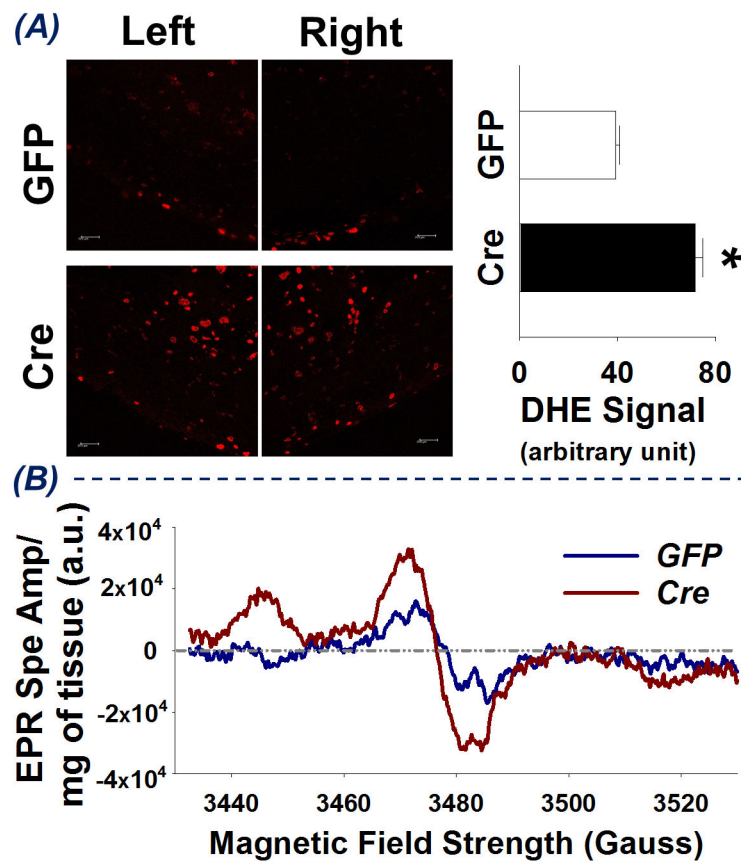


Figure 3. Superoxide levels in the RVLM of mice following bilateral microinjection of Lentiviral-GFP (GFP) or Lentiviral-Cre-GFP (Cre). (A) left - DHE staining images of brainstem sections at 1.9 mm caudal to lambda; right- the quantified density of red fluorescence, *P < 0.05 vs GFP-mice, n = 6 for each group. (B) EPR spectra obtained from pooled RVLM punches from 8 mice, 4 GFP-mice and 4 Cre-mice. (a.u. = arbitrary units)

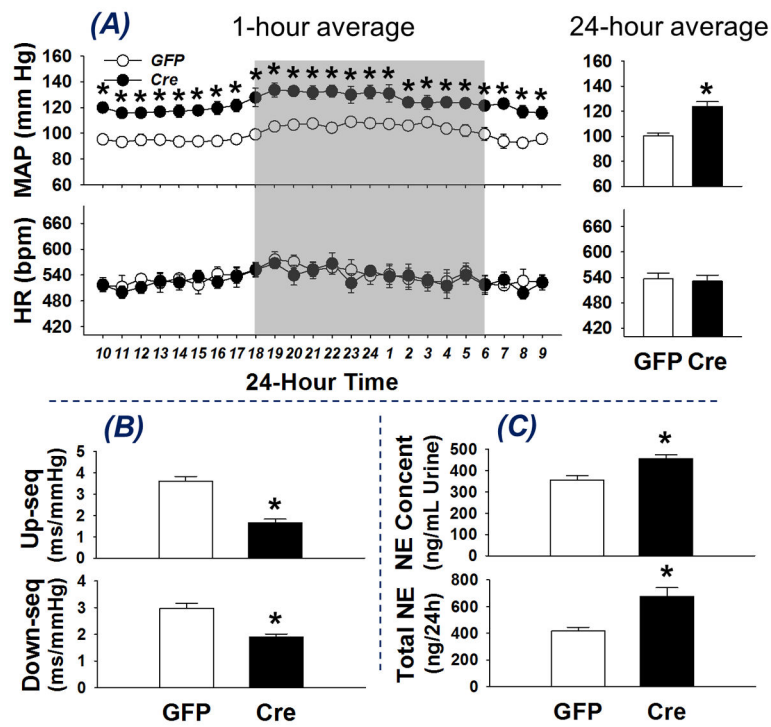


Figure 4. Blood pressure and heart rate (A), spontaneous arterial baroreflex sensitivity (B), and urinary norepinephrine excretion (C) in conscious mice with bilateral microinjection of Lentiviral-GFP (GFP) or Lentiviral-Cre-GFP (Cre). * $P < 0.05$ compared with GFP mice, $n = 6$ for each group.

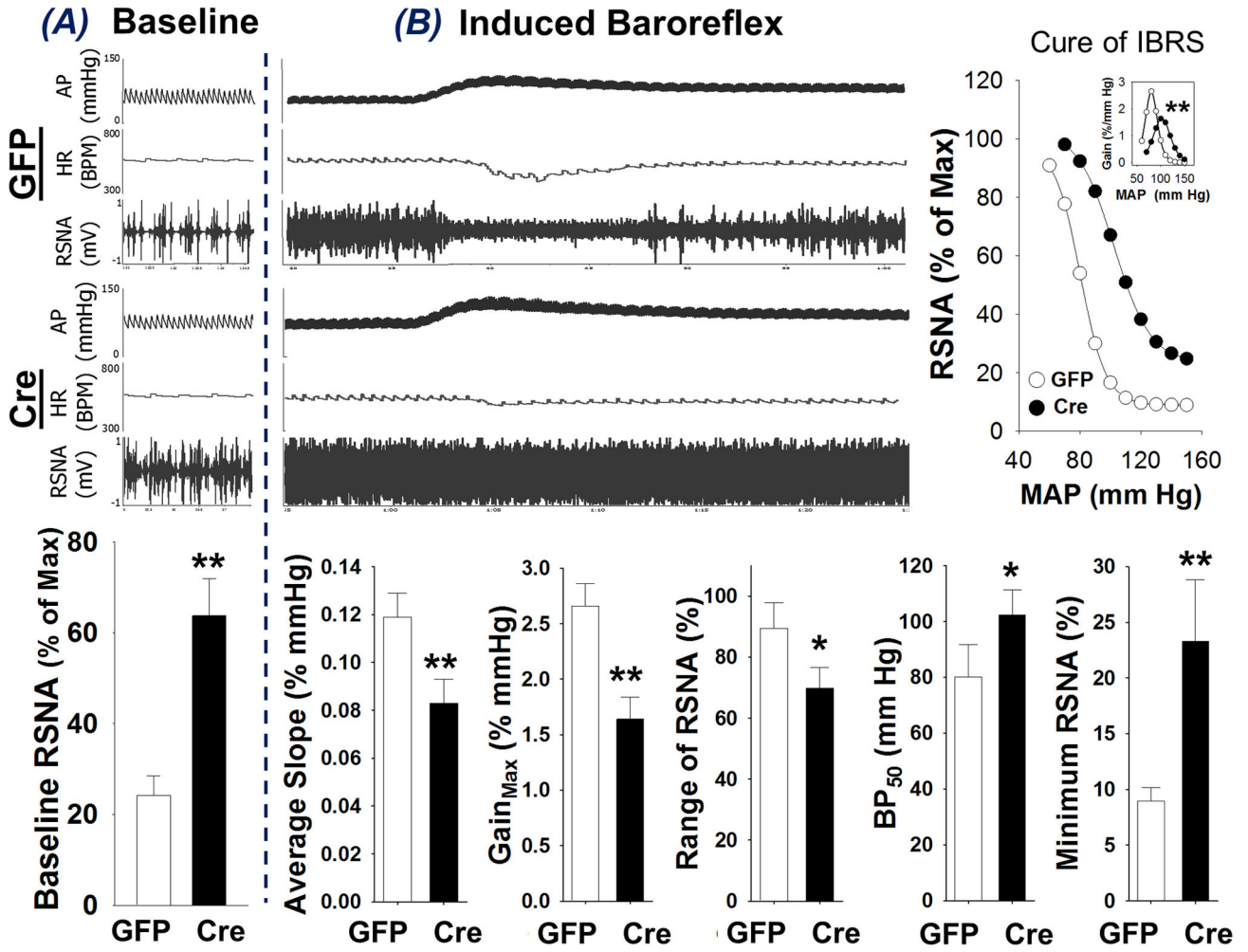


Figure 5. Baseline renal sympathetic nerve activity (RSNA, A) and induced arterial baroreflex sensitivity (IBRS, B) in anesthetized mice with bilateral microinjection of Lentiviral-GFP (GFP) or Lentiviral-Cre-GFP (Cre). *P < 0.05 and **P < 0.01 compared with GFP mice, n = 6 for each group.